Digest Journal of Nanomaterials and Biostructures Vol. 11, No. 3, July - September 2016, p. 1007 - 1016

DIFFERENT SUBSTRATES EFFECTS ON THE TOPOGRAPHY AND THE STRUCTURE OF THE ZnO NANORODS GROWN BY CHEMICAL BATH DEPOSITION METHOD

A. F. ABDULRAHMAN[a*], S. M. AHMED[b], N. M. AHMED[c], M. A. ALMESSIERE[d]
[a]*Physics Department, Faculty of Science, University of Zakho, Zakho, Kurdistan Region, Iraq*
[b]*Physics Department, Collage of Science, University of Dohuk, Dohuk, Kurdistan Region, Iraq*
[c]*Nano-Optoelectronic Research & Technology Laboratory, School of Physics, University Sains Malaysia, Penang, Malaysia*
[d]*Physics Department, Collage of Science, University of Dammam, Dammam, Kingdom of Saudi Arabia*

In this paper, vertically aligned ZnO nanorods arrays were fabricated on different substrates. The substrates are Indium Tin Oxide (ITO) coated glass, polyethylene terephthalate (PET), Silicon (Si), Porous Silicon (PS) and Kapton Tape (KT). Nanorods are fabricated at low temperature by using chemical bath deposition method. The investigation of the effect of substrates on the morphological, elementary composition and structural characteristics of ZnO nanorods has been done. Field emission scanning electron microscopy (FESEM), Energy Dispersive analysis (EDX) and X-ray diffraction (XRD) measurements were used to investigate the morphological, compositional and structural characteristics with hexagonal wurtzite structure of the ZnO nanorods arrays. The average diameter of ZnO nanorods are found to be closely related to the substrates nature. It is concluded that the substrates can effect on the ZnO nanorods growth remarkably and the selective growth of ZnO nanorods is possible through the choice of the substrates. The crystallite size and the lattice constants of the synthesis ZnO nanorods were calculated based on the XRD data. The found results revealed that the increase in the crystallite size is strongly associated with the type of substrate.

(Received August 3, 2016; Accepted September 28, 2016)

Keywords: ZnO, CBD, Nanostructure, Nanorods, Different substrates, ITO, PET, Porous Silicon, Silicon, Kapton Tape

1. Introduction

One dimensional (1 D) Zinc oxide (ZnO), which is an important electronic and photonic material with large direct band gap (3.37 eV)semiconductor [1], thermal and excellent chemical stability , biocompatibility transparency, large electrical conductivity range [2] and wide exciton binding energy (60 meV) at room temperature [3]. These properties make ZnO a more promising material in excitonic emissions and lasing applications above room temperature compared with other materials. In addition to its chemicals and thermal properties, ZnO also has piezoelectric and photo conducting characteristics. Thus, it has potential for a wide range of applications, such as for UV optical devices, LED, biomedical applications, gas sensing, and solar cells [4-8].

ZnO nanostructure films such nanorods, nanotube, nanowire, nanocrystal, nanodisks, nanosheet [9-14] and so on have a large range of technological applications including field emitters [15],gas sensors [16], dye-sensitized solar cells [17], optoelectronics [18]and in biological application [19].

*Corresponding author: ahmadamedi@yahoo.com

In the literature, many synthesis methods have been introduced for the preparation of a variety of ZnO nanorods on a large range of substrates [20]. These methods include chemical vapor deposition (CVD) [21], metallic organic chemical vapor deposition (MOCVD) [22], electrochemical deposition [23], pulsed laser deposition [24], radiofrequency magnetron sputtering [25], vapor phase transport [26] and spray pyrolysis [27]. Among these methods mention above, the chemical bath deposition (CBD) method is a low temperature method and possibly the lowest cost method for growing ZnO nanorods not need the high production yield.

In previous works, studied were mainly focused on the preparation of the ZnO nanorods and growth conditions and solution parameters such as temperature, time, concentration on the morphology and the structure of the ZnO nanorods. Also substrates can also effect on the growth of the ZnO nanorods because the surface topography and structure of substrates and their lattice mismatch with nanostructure are particular significant parameters since these factors control the morphology and nature of synthesis ZnO nanorods. The investigation of a substrate effect can help us to help growth mechanisms. In addition, an understanding of the substrate effect has the potential parameter to realize the selective growth of nanomaterials, which are very useful for future nano electronics, nano devices and nano sensors [28].

In this paper, five types of substrates (flexible and non-flexible) including Indium Tin Oxide (ITO) coated glass, polyethylene terephthalate (PET), Silicon (Si), Porous Silicon (PS) and Kapton Tape (KT) were selected and study the growth characteristic such as morphology and structure of ZnO nanorods on these substrates. The experimental results found that the quantity and quality of ZnO nanorods produced on these different substrates were very different.

2. Experimental details

All chemicals were of analytical grade from Sigma Aldrich Company, and were used as starting materials without further purification. In this experiment, ZnO seed layer coated on different substrates such as (ITO, PET, Kapton Tape, Silicon and Porous Silicon) were employed as a substrate for growing ZnO nanorods. This process was performed in two stages.

In the first stage: cleaning the different substrates, the ITO coated glass substrates were cleaned in an ultrasonic bath by using ethanol, acetone and deionized water for 15 min respectively and dried with nitrogen gas. The PET substrates cleaned by using 2-propanol and acetone to remove any contamination and dried with nitrogen gas. The Kapton Tape was fixed onto a microscope slide glass (75* 24*1.2 mm) substrate and cleaned by using 2-propanol and acetone to remove any contamination and dried with Nitrogen gas. Then, the n-type Si (100) and Porous silicon (100) substrates were cut into squares with dimensions of 13 mm * 13 mm using a diamond cutter machine. Prior to creating the silicon and PS layer, the standard cleaning procedure was employed to remove the oxide layer and other contamination from the surface of the prepared Si and PS substrates. The Radio Corporation of America (RCA) prescribes three successive steps for cleaning of these types of substrates. The first step is removing the organic contaminations by immersing the Si substrates in $H_2O + H_2O_2 + NH_4OH$ solution at a ratio 5:1:1 at 80 °C for 10 min. the second step is removing the thin oxide layer by immersion in H_2O + HF solution with at a ratio of 50:1 for 20 sec at room temperature. The final step is removing the ionic atomic contaminations using $H_2O + H_2O_2$ + HCl solution at a ratio of 6:1:1 at 80 °C for 10 min and Si substrates were rinsed in DI water and dried in Nitrogen gas. The PS layer was prepared from n-type Si (100) wafer by the PECE method. The PECE process was conducted in a Teflon cell. The electrolyte consisted of 4:1 volume ratio mixture of ethanol (96%) and hydrofluoric acid (48%). The PS layer was formed with a constant current density of 2 mA for 20 min at room temperature using the Pt wire and Si as the cathode and a respectively. The sample was illuminated with a 60 W visible lamp during etching process. The prepared PS Substrates were rinsed with DI water and the dried with nitrogen gas after etching.

In the second stage, a radio frequency magnetron sputtering was employed using target (99.999% purity) to deposit ZnO seed layer on the cleaned different substrates (ITO, PET, Kapton tape, silicon and porous silicon). The 100 nm thick ZnO seed layer was deposited on the different substrates with argon gas with pressure 5.5 $*10^{-3}$ mbar and RF sputtering power 150 Watt for 15

min. After that ZnO seed layer coated on the different substrates were placed in an annealing tube furnace at 200^{o}C for 1 h to improve the structural quality and optical properties of the ZnO seed layer.

2.1 Growth Process

For vertical aligned growth of ZnO nanorods on the seed layer of ZnO different substrates (ITO, PET, Kapton tape, silicon and porous silicon) using the low temperature CBD method, hexamethylenetetramine ($C_6H_{12}N_4$) and zinc nitrate hexahydrate ($Zn(NO_3)_2.6H_2O$) was employed as precursors and deionized water was used as a solvent. A suitable amount of ($Zn(NO_3)_2.6H_2O$) equal molar concentration of ($C_6H_{12}N_4$) was separately dissolved in deionized water at 80 ^{o}C and mixed together under magnetic stirrer. The prepared substrates were inserted vertically inside a beaker including a mixture of the two solutions. To investigate the influence of different substrates on the morphology and structure of ZnO nanorods, the beaker was placed inside an oven at 95^{o}C for 4 h. After complete the growth of the ZnO nanorods, the substrates was first taken out from a solution and washed with deionized water to remove the remaining salt, and then it was dried with nitrogen gas.

2.2 Characterization techniques

The FESEM images (diameter of ZnO nanorods), distribution and homogeneity of ZnO nanorods and energy dispersive X-ray spectroscopy (EDX) analysis to provide qualitative and quantitative analyses of elemental composition of the samples were studied. The model of FESEM used in this study is: FEI Nova nano SEM 450 (The Netherlands), and Leo-Supra 50 VP, Carl Zeiss (Germany). Also in this study a high resolution XRD (HR-XRD) system X-Pert Pro MRD model with CuKα (λ = 0.154050 nm) radiation and scanning range of 2θ set between 20˚ and 80˚ was used to characterize the crystal structure, the strain, and the quality of the epitaxial growth of ZnO nanorods on the different substrates.

3. Result and discussion

3.1 Morphological Analysis of ZnO Nanorods

Fig. (1) shows the FESEM images of ZnO nanorods prepared by chemical bath deposition (CBD) on the different substrates such as (ITO, PET, Porous Silicon, Silicon and Kapton Tape) at 95 °C for 4 h. Figure 1 (a) shows the ZnO nanorods grown on seeded Indium Tin Oxide (ITO), it was observed that the nucleation of ZnO nanorods occurred on the surface of the seed layer and the distribution of the nanorods was randomly oriented and ZnO nanorods has no vertically aligned on the ITO substrates. But in the figure 1 (b) one can see that the ZnO nanorods grown on the PET was well vertically aligned and uniformly orientated. Also figure 1 (c) shows ZnO well-defined nanorods arrays and were successfully grown vertically on porous silicon. It can be clearly observed from the figure 1 (c) that the ZnO nanorods like nanoflowers and have no hexagonal shape. Also it can be seen that the bottom of the ZnO nanorods is smaller than the top of the ZnO nanorods and one can believe that the PS layer produces a large mismatch in lattice constants and thermal expansion coefficients, thereby producing a large stress between ZnO nanostructures and PS substrates [29]. Figure 1 (d) shows the well vertically aligned ZnO nanorods along the c-axis with a high distribution density of nanorods over the entire silicon substrate, it can be seen that the orientation of ZnO nanorods is uniform and have a hexagonal shape. In addition figure 1 (f) shows the vertically aligned ZnO nanorods along the c-axis with a high distribution density of nanorods over the entire Kapton tape substrate, it can be seen that the orientation of ZnO nanorods is randomly and have nanorods and nanotube, and also it can clearly observed that they have raindrop over most of the ZnO nanorods and this is may be due to the substrate effect (Kapton tape) on the growth way of nanorods on this type of substrate.

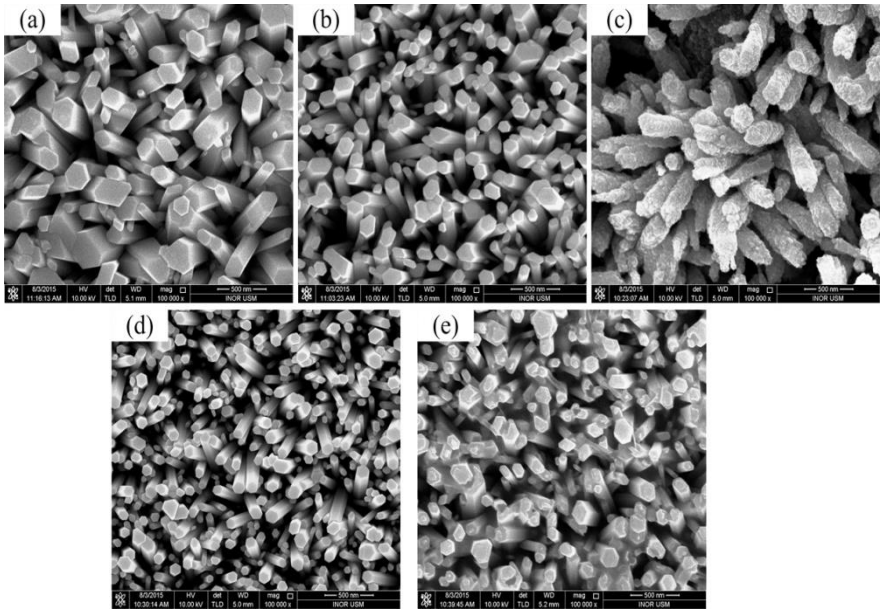

Fig (1) FESEM images of ZnO nanorods on different substrates: (a). ITO, (b). PET, (c) Porous Silicon, (d) Silicon and (f) Kapton Tape

Fig. 2 shows the average diameter of ZnO nanorods prepared by the chemical bath deposition (CBD) method on the different substrates. It can clearly observed that the average diameter of the ZnO nanorods grown on ITO is (234.4 nm) which is larger than the nanorods prepared on Kapton tape substrate (182.4 nm) and the diameter is decreases according to the type of substrate (nanorods diameter prepared on PET is (169.7nm), for porous silicon nanorods is (165 nm) and for silicon substrate is (99.59 nm)). From the figure one can believe that the substrate playing a major role in determining the nanorods diameter. This nanorods diameter dependence on the type of substrate and this can be related to the fact that the surface topography and structure of substrates and their lattice mismatch with nanostructure have particular significant parameters on nanorods diameter since these factors control the morphology and nature of synthesis ZnO nanorods. The investigation of a substrate effect can help us to probe growth mechanisms [28].

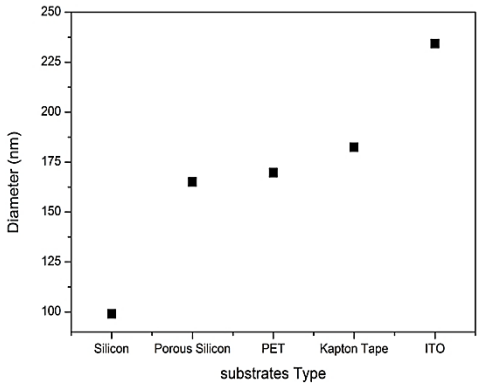

Fig. 2. Average diameter of ZnO nanorods versos different substrates.

3.2 Energy Dispersive X-Ray Analysis (EDX):

The composition of the as-grown ZnO nanorods synthesis at 95 ^{o}C for 4 h on the different substrates was performed by EDX analysis. Figure 3 shows the corresponding EDX analysis which reveals the existence of Zn and O, which corresponds to the characteristic composition of ZnO, without the presence of any impurities or substrate signal according to EDX limitations. The

ratio between Zn and O was the same for all analyzed samples grown on different substrates. Figure 3 (a, b), it can be notice that the elementary chemical compositions for the grown nanorods are zinc and oxygen only. The molecular ratio of Zn:O of the grown nanorods calculated from quantitative EDX analysis data, is close to that of 1:1. The EDX spectrum confirmed that the grown nanorods are pure ZnO but elementary composition data of the substrates not detected by EDX test because of the densely growth of the ZnO nanorods.

Also figure 3 (c, d & f) shows the quantitative EDX analysis for the nanorods prepared by CBD on Porous silicon, silicon and Kapton tape substrates respectively. The EDX spectrum confirmed also that the grown nanorods are pure ZnO and quantitative analysis data, is close to that of 1:1, and also the spectrum of these three substrates is appeared, and this is because of the topography, structure and nature of the substrates effect on the ZnO nanorods growth produces not dense ZnO nanorods which have small space between the nanorods. This space give chance to the high energetic electrons of the FESEM to interact with the substrate and produces XRF coming from the constituents of the surface of the substrate.

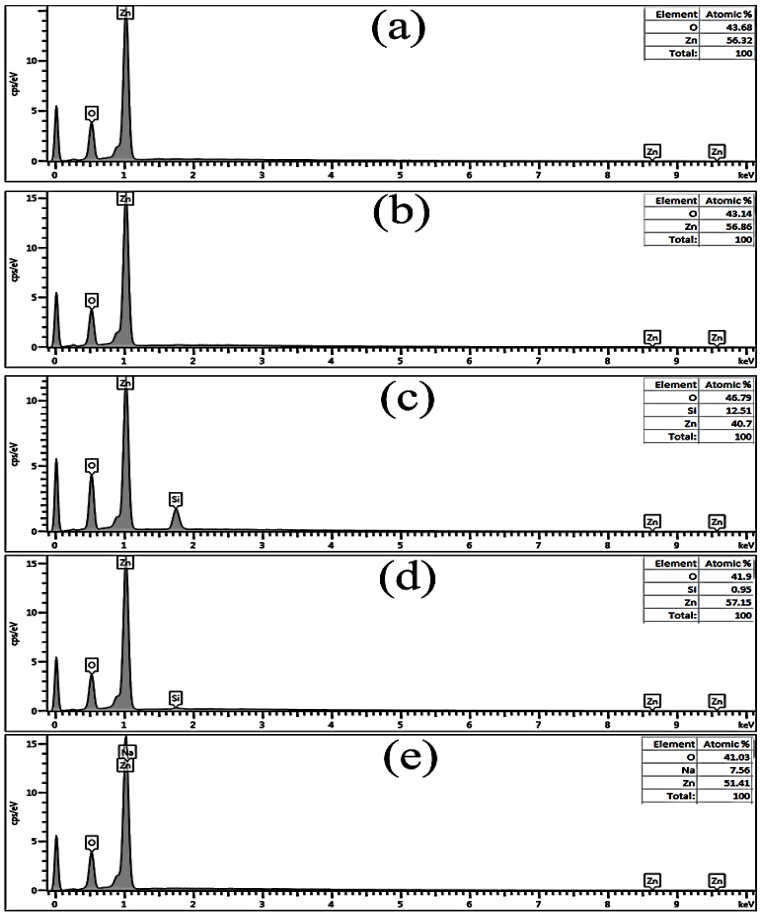

Fig. (3) EDX analysis with it quantity that the grown ZnO nanorods on different substrates: (a). ITO, (b). PET, (c) Porous Silicon, (d) Silicon and (f) Kapton Tape

3.3 Structural Characteristics

The X-Ray diffraction (XRD) patterns of ZnO nanorods grown on different substrates including Indium Tin Oxide (ITO) coated glass, polyethylene terephthalate (PET), Silicon (Si), Porous Silicon (PS) and Kapton Tape (KT) are displayed in figure 4. It can clearly see that the ZnO nanorods that grown on all the five substrates have a wurtzite hexagonal structure with a strong diffraction intensity peak related to the (0 0 2) plane. This is indicating that they have a c-axis orientation perpendicular to the all substrates, which can be indexed to a standard spectrum in the ICSD database (No. 01-071-6424). Figure 4 (a) shows the X-ray diffraction pattern of the ZnO

nanorods grown on Indium Tin Oxide (ITO) coated glass substrate, it reveals that the several peaks of the hexagonal structure of ZnO nanorods, such as (002),(100),(101), (103) and (103) are appeared and the inset peak is diffracted from the (0 0 2) plane of the ZnO nanorods (2θ= 34.5671) which is represent the 100% of ZnO hexagonal structure, and also the diffracted peaks belong to the substrate are appeared in the XRD pattern. Figure 4 (b) shows that the XRD pattern of the ZnO nanorods grown on PET, it can clearly seen that the (002) diffracted peak of ZnO nanorods (2 θ = 34.4772) in XRD pattern is dominant, and other peaks which diffracted from other planes are too small, which reveals the preferentially oriented growth in the c-axis direction. In addition the diffracted peaks belong to the PET substrate are appeared in the XRD pattern.

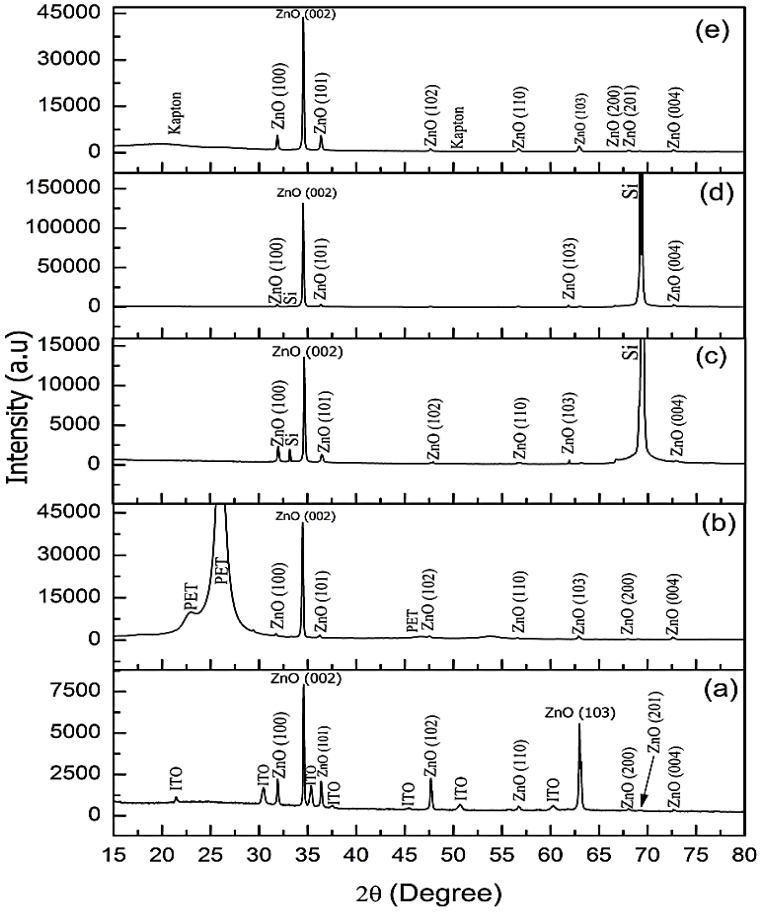

Fig. 4 X-Ray diffraction patterns ZnO nanorods on different substrates: (a). ITO, (b). PET, (c) Porous Silicon, (d) Silicon and (f) Kapton Tape

Fig. 4 (c) shows that the X-ray diffraction pattern of the ZnO nanorods grown on the porous silicon substrate prepared by CBD method, it is observed that the diffraction peaks have high intensity (002) with (2θ =34.6535), (100) and (101) plans and other peaks which diffracted from other planes are too small, which reveals the preferentially oriented growth in the c-axis direction, and also the diffracted peaks belong to the porous silicon substrate are appeared in the XRD pattern. The crystal structure of the as-grown ZnO nanorods prepared in CBD process grown on silicon substrate the XRD pattern as shown in figure 4 (d). It is observed that the as-grown ZnO nanorods are hexagonal structure, the remarkably sharp peak at (2θ= 34.5125) is assigned to be the (002) peak of hexagonal, the strong and narrow indicates that the as-grown sample have good crystallinity and preferentially oriented along the c-axis as well as perpendicular to the substrate surface which is well in agreement with the FESEM image and expect for the peak located at (2 θ of 69.2612) which was related to the silicon substrate. In addition, the crystal structure of ZnO nanorods grown on the Kapton Tape at low temperature the X-ray diffraction pattern as shown in

figure 4 (f), it can clearly see that the all the diffraction beaks (002) at (2θ= 34.5358), (100) and (101) plans in the pattern have been indexed as the hexagonal phase of ZnO nanorods. In addition the diffracted peaks belong to the Kapton tape substrate are appeared in the XRD pattern.

The one most often used approaches in estimating the average particle size of the X-ray data is the utilization of the Debye Scherer formula [30]:

$$D = \frac{K\lambda}{\beta cos\theta} \quad (1)$$

Where k is a constant which is taken to be 0.9, λ is the wavelength of the X-ray used (0.154056 nm), β is the full width at half maximum of the peak and the θ is the Braggs diffraction angle.
The types of substrate and growth conditions are affected on the increase and decrease in the crystallite size (average particle size). In the table 1 and figure 4, it shows that the crystallite sizes were 115.555, 57.7635, 69.3494, 69.3228 and 57.7726 nm for the ZnO nanorods grown on ITO, PET, Porous silicon, silicon and Kapton tape substrates, respectively. This variation in crystallite size (average particle size) can clearly be observed in the X-ray diffraction (XRD) pattern shown in Figure 4 as an increase and decrease in the FWHM of the ZnO peaks. The dependence of the D values on the type of substrate can be attributed to both lattice and thermal mismatching between these different substrates and ZnO nanorods. In table 1, it can note that the FWHM of silicon and porous silicon are same value because they have the same thermal mismatching, lattice parameters and they are same material. For PET and Kapton Tape which are also reflect the same crystallite size and this is because the two types are polyimide and the same reasons mentioned above (for silicon and porous silicon) can be considered to explain this.

The dislocation density (δ), which represents the amount of defects in the crystal, is estimated from the following equation [31]:

$$\delta = \frac{1}{D^2} \quad (2)$$

Where D is the crystallite size.

In equation 2, the dislocation of density depended inversely square on the crystallite size, it means that the crystallite size of ZnO nanorods grown on ITO substrate is higher than the porous silicon to silicon to Kapton tape to PET substrates, then the dislocation density of ZnO nanorods grown on ITO is smaller than the dislocation density of ZnO nanorods on Porous silicon to silicon to Kapton tape to PET substrates as shown in table 1, i.e. the amount of defects in the crystal of ZnO nanorod grown on ITO substrate that less than the grown on PET substrate.

Table 1. Lattice parameters and Structure properties of the ZnO nanorods grown on different substrates: (a). ITO, (b). PET, (c) Porous Silicon, (d) Silicon and (f) Kapton Tape

Substrates	plan	Intensity	a(Å)	c (Å)	d (Å)	$2\theta^o$	FWHM(β)^o	ξ_a %	D (nm)	δ(Å)$^{-2}$
ITO	002	7867	2.99381	5.18545	2.59272	34.5671	0.072	-7.86549	115.555	$7.48896*10^{-7}$
PET	002	42657	3.00138	5.19856	2.59928	34.4772	0.144	-7.63256	57.7635	$2.99705*10^{-6}$
PS	002	13959	2.98658	5.17291	2.58646	34.6535	0.120	-8.08818	69.3494	$2.07929*10^{-6}$
Si	002	133585	2.99841	5.19340	2.59670	34.5125	0.120	-7.72417	69.3228	$2.08088*10^{-6}$
Kapton	002	44379	2.99644	5.19000	2.59500	34.5358	0.144	-7.78453	57.7726	$2.99609*10^{-6}$

The lattice constants a and c of the ZnO wurtzite structure can be calculated using Bragg's law, as it's shown in table 1, [32, 33]:

$$a = \sqrt{\frac{1}{3}}\ \frac{\lambda}{sin\theta} \tag{3}$$

$$c = \frac{\lambda}{sin\theta} \tag{4}$$

Where λ = 0.15405 nm is the wavelength of the X-ray source and θ is the angle of the diffraction peak.

The strain (ε_c) of the ZnO nanorod grown on the glass substrate along c-axis can be calculated by using the following equation [34-36]:

$$\Sigma_c = \frac{c-c_o}{c_o} * 100\% \tag{5}$$

The perpendicular strain (ε_a) along the a-axis ZnO nanorod grown on the different substrates can be calculated using the following equation [37]:

$$\Sigma_a = \frac{a-a_o}{a_o} * 100\% \tag{6}$$

Where c_o and a_o are represents the standard lattice constants for unstrained ZnO nanorods which are equal to (c_o =5.2038 Å) and (a_o = 3.2494 Å) obtained from the X-ray diffraction pattern data and the standard lattice constant for unstrained ZnO nanorods ICSD database (No. 01-071-6424). The values of ε_a are positive for the tensile strain indicated in lattice constant that and negative for the compressive strain that indicated in lattice constant, the values of lattice parameters (a, c) are shown in table 1.

In table 1, it shows that the values of the perpendicular strain (ε_a) along the a-axis ZnO nanorod grown on the different substrates such as ITO, PET, Porous Silicon, Silicon and Kapton tape substrates are indicated the compressive strain that indicated in lattice constant. These values generally depended on the lattice parameters (a, a_o) that depend on the plane spacing (d) and angle (θ) or (2θ). For example the perpendicular strain ε_a (compressive strain) were -7.86549 %, -7.63256 %, -8.08818 %, -7.72417 % and -7.78453 % for the ZnO nanorods grown on ITO, PET, Porous silicon, silicon and Kapton tape substrates, respectively. This variation is due to the can clearly be observed in the X-ray diffraction (XRD) pattern shown in Figure 4 as an increase and decrease in the 2θ of the ZnO peaks and variation on a values shown in table 1, it can found from table 1 the perpendicular strain (ε_a) along the a-axis ZnO nanorod grown on porous silicon higher than the ITO to Kapton tape to PET to Silicon because to the variation of (2θ) and values of lattice constant (a), i.e. the 2θ of ZnO nanorods grown on Porous silicon is higher and lattice parameters (a) is lower for porous silicon.

The lattice constant (a) and (c) of wurtzite hexagonal structure zinc oxide is calculated according to Braggs law Equation 1and the equation 2 which is related to plane spacing and miller indices [32]:

$$2dsin\theta = n\lambda \tag{7}$$

Where d in the plane spacing, n is the order of diffraction that usually is 1, λ is x-ray wavelength. In table 1, it can clearly note that the plane spacing (d) of ZnO nanorods grown on different substrate have the variation values because of the nature and surface topography and structure of substrate and their lattice mismatch with nanostructure are particular significant parameters since these factors control the morphology and nature of synthesis ZnO nanorods. Its appear from the table 1 that the value of plane spacing (d) of ZnO nanorods grown on porous substrate and on silicon is high and less respectively, and plane spacing have less than compared to the plane spacing that indicated from the unstrained ZnO nanorod as ICSD database (No. 01-071-6424), because to the large mismatching and lattice constant between the ZnO nanorods and substrates.

4. Conclusions

In summary, ZnO nanorod arrays were successfully synthesized by chemical bath deposition (CBD) method on different substrates ITO, PET, Porous silicon, silicon and Kapton tape at same growth conditions. Effects of the substrate on the morphology and structure of ZnO nanorods were studied. FESEM and XRD results demonstrate that the ZnO nanorod arrays with a hexagonal wurtzite structure were grown densely and vertically aligned on all the substrates, whereas the average diameter was found to be closely related to the substrates nature. The ZnO nanorods grown on ITO substrates showed an average diameter of 234.4 nm, while those grown on PET substrates had an average diameter of 169.7nm, but average diameter of ZnO NRs grown on porous silicon is 165nm, on the silicon is 99,59 nm and Kapton tape had average diameter of 182.4 nm. The obtained crystallite size revealed that the increase in the crystallite size is strongly associated with a minor dependence on the type of the substrate. From XRD results, approve the surface topography and structure of substrates and their lattice mismatch with nanostructure are particular significant parameters since these factors control the morphology and nature of synthesis ZnO nanorod by have shift in d-spacing. The high intensity as a peak is observed corresponding to ZnO nanorods (002) plan, revealing the preferentially oriented growth along the c-axis grown on silicon substrate is 133585, for Kapton tape is 44379, for PET is 42657, for porous silicon is 13959 and on ITO is 7867.

References

[1] H. Morkoc, U. Ozgur, Wiley-VCH Verlag GmbH & Co. KGaA, 2009, pp. 1.
[2] P. Suresh Kumar, M. Yogeshwari, A. Dhayal Raj, D. Mangalaraj, D. Nataraj, U. Pal, Journal of Nano Research **5,** 223 (2009).
[3] Kyung Ho Kim, Kazuomi Utashiro, Yoshio Abe, and Midori Kawamura, Int. J. Electrochem. Sci. **9**, 2014.
[4] S.S. Shinde, K.Y. Rajpure, Appl. Surf. Sci. **257,** 9595 (2011).
[5] Y. Ryu, T.S. Lee, B.J. Kim, Y.S. Park, C.J. Youn, Appl. Phys. Lett. **88,** 241108-1 (2006).
[6] A.I. Hochbaum, P. Yang, Chem. Rev. 110, 527 (2010).
[7] L.Hey-Jin, Y. L.Deuk, O. Young, Sensors and Actuators A: Physical, **125**(2), 405 (2006).
[8] R Marte, T Schmidt, H R Shea, et al. Appl. Phys. Lett. **73**(17): 2447 (1998)
[9] Z. Zhang, H. Yu, Y. Wang, M.Y. Han, Nanotechnology, **17,** 2994 (2006).
[10] Q. Li, V. Kumar, Y. Li, H. Zhang, T.J. Marks, and R.P. H. Chang, Chem. Mater. **17,** 1001 (2005).
[11] J.H. Shin, J. Y. Song, H.M. Park, Mater. Lett. **63,** 145 (2009).
[12] J.J. Cole, X. Wang, R.J. Knuesel, H.O. Jacobs, Adv. Mater. **20,** 1474 (2008).
[13] P. X. Gao, C.S. Lao, Y. Ding, Z.L. Wang, Adv. Funct. Mater. **16**, 53 (2006).
[14] S. Chen,Y. Liu, C. Shao, R. Mu,Y. Lu,J. Zhang, D. Shen, X. Fan, Adv. Mater. **17,** 586 (2005).
[15] H. Hu, K. Yu, J. Zhu, Z. Zhu, Appl. Surf. Sci. **252,** 8410 (2006).
[16] T. Gao, T.H. Wang, Appl. Phys. A: Mater. Sci. Process. **80,** 7 (2005).
[17] J.B. Baxter, A.M. Walker, K.V. Ommering, E. Saydil, Nanotechnology **17,** S304 (2006).
[18] X. Wang, C.J. Summers, Z.L. Wang, Nano Lett. **4**(3) 423 (2004).
[19] T.Y. Liu, H.C. Liao, C.C. Lin, S.H. Hu and S.Y. Chen, Langmuir **22,** 5804 (2006).
[20] Huang, T. H., C., Mitch, M.C., UWE, J., Formation mechanism of {0001} ZnO epitaxial layer on γ-LiAlO2 (100) substrate by chemical vapor deposition semiconductor devices, materials and processing, J. Electrochem. Soc. **158**, H38 (2011).
[21] P. Yang, H. Yan, S. Mao, R. Russo, J. Johnson, R. Saykally, N. Morris, J. Pham, R. He, H.-J. Choi, Adv. Funct. Mater. **12,** 323 (2002).
[22] D. Montenegro, V. Hortelano, O. Martinez, M. Martínez Tomas, V. Sallet,V. Muñoz-Sanjosé, J. Jiménez, J. Appl. Phys. **113,** 143513 (2013).
[23] H H Guo, J Z Zhou, Z H Lin. Electrochem. Commun. **10**(1), 146 (2008).
[24] J.H. Choi, H. Tabata, T. Kawai, J. Cryst. Growth **226**, 493 (2001).
[25] J.Y. Lee, Y.S. Choi, J.H. Kim, M.O. Park, S. Im, Thin Solid Films **403**, 553 (2002).

[26] Xu, C. X.; Sun, X. W.; Dong, Z. L.; Yu, M. B. Appl. Phys. Lett. **85**, 3878 (2004). doi:10.1063/1.1811380
[27] M.G. Ambia, M.N. Islam, M.O. Hakim, J. Mater. Sci. **29**, 6575 (1994).
[28] X.H. Wang, J. Zhang and Z.Q. Zhu, Applied Surface Science, **252(**6), 2404 (2006).
[29] R. Shabannia, H. Abu Hassan, Supperlattices Microstruct. **62**, 242 (2013).
[30] B.D.Cullity, Elements of X-ray Diffraction, second edition, Addison Wesley (2007).
[31] A.H. Kurda, Y. M. Hassan, N. M. Ahmed, World Journal of Nano Science and Engineering, **5**, 34 (2015)
[32] M. Kashif, U. Hashim, M. E. Ali, Syed M. Usman Ali, M. Rusop, Z. H. Ibupoto, M. Willander, Hindawi Publishing Corporation Journal of Nanomaterials ,V. 2012, Article ID 452407, 6 pages.
[33] C Suryanarayana, G Norton, X-Ray Diffraction: A Practical Approach. Springer Science + Business Media, LLC, 233 Spring Street, New York, NY 10013, USA: Plenum Press; 1998.
[34] B.E. Warren, X-ray Diffraction (Courier Dover Publications, New York, 1969).
[35] H. Lipson, Contemp. Phys. **20**, 87 (1979).
[36] C.-Y. Tsay, K.-S. Fan, S.-H. Chen, C.-H. Tsai, J. Alloys Compd. **495**, 126 (2010).
[37] J. Kühnle, R. B. Bergmann, J. H. Werner, J. Cryst. Growth, **173**, 62 (1997) doi:10.1016/S0022-0248(96)00783-X.